

Novel mutations in *LTBP2* identified in familial cases of primary congenital glaucoma

Bushra Rauf,^{1,2} Bushra Irum,^{1,2} Shahid Y. Khan,¹ Firoz Kabir,¹ Muhammad Asif Naeem,² Sheikh Riazuddin,^{2,3} Radha Ayyagari,⁴ S. Amer Riazuddin¹

¹The Wilmer Eye Institute, Johns Hopkins University School of Medicine, Baltimore, MD; ²National Centre of Excellence in Molecular Biology, University of the Punjab, Lahore, Pakistan; ³Allama Iqbal Medical College, University of Health Sciences, Lahore, Pakistan; ⁴Shiley Eye Institute, University of California San Diego, La Jolla, CA

Purpose: Primary congenital glaucoma (PCG) is a genetically heterogeneous disorder caused by developmental defects in the anterior chamber and trabecular meshwork. This disease is an important cause of childhood blindness. In this study, we aim to identify the genetic determinants of PCG in three consanguineous families of Pakistani descent.

Methods: Affected members of all three families underwent detailed ophthalmological examination including slit-lamp biomicroscopy. Blood samples were collected from affected and healthy members of all three families, and genomic DNA was extracted. Linkage analysis was performed for the known or reported loci of PCG to localize the disease interval, and logarithm of odds (LOD) scores were calculated. All protein-coding exons of the candidate gene, latent transforming growth factor-beta binding protein 2 (*LTBP2*), were bidirectionally sequenced to identify the disease-causing mutation.

Results: Short tandem repeat (STR) marker-based linkage analysis localized the critical interval to chromosome 14q with a maximum two-point LOD score of 2.86 (PKGL076), 2.8 (PKGL015), and 2.92 (PKGL042). Bidirectional Sanger sequencing of *LTBP2* revealed three novel pathogenic variants, i.e., c.3028G>A (p.Asp1010Asn), c.3427delC (p.Gln1143Argfs*35), and c.5270G>A (p.Cys1757Tyr) in PKGL076, PKGL015, and PKGL042, respectively. All three mutations segregated with the disease phenotype in their respective families and were absent in 200 ethnically matched normal chromosomes.

Conclusions: We identified three novel mutations, p.D1010N, p.Q1143Rfs*35, and p.C1757Y, in *LTBP2* responsible for PCG.

The term glaucoma represents a heterogeneous group of neurodegenerative disorders that have a specific type of optic neuropathy, causing irreversible defects in the visual field. The disease is deceptive, and sometimes, individuals remain undertreated or undiagnosed because central vision is usually not lost at an early stage of the disease [1,2]. Glaucoma is the second leading cause of blindness accounting for nearly 12.3% cases of visual loss worldwide [1,2].

Primary congenital glaucoma (PCG; OMIM 231300), a severe type of glaucoma, is characterized by developmental defects in the trabecular meshwork (trabeculodysgenesis) with neonatal or infantile onset [3]. Genetic defects in the trabecular meshwork are responsible for various forms of glaucoma [4]. The classical triad of symptoms presented by PCG is photophobia (hypersensitivity to light), epiphora (excessive tearing), and blepharospasm (inflammation of eyelids) [5]. Other clinical findings include Haab's striae (rupture of Descemet's membrane), elevated intraocular pressure (IOP), buphthalmos, conjunctival erythema, corneal

edema, and optic atrophy in later stages of the disease [6-9]. It is a rare form of glaucoma representing 1% to 5% of all cases of glaucoma [10]. Although sporadic cases of PCG are more common, familial cases have also been documented. In familial cases, PCG is normally inherited in an autosomal recessive pattern with incomplete penetrance, but recently, an autosomal dominant inheritance case was reported [3,11,12].

As the molecular etiology of PCG is not fully understood, only a few genes responsible for the disease are known [13-18]. Four chromosomal locations, GLC3A (2p22-p21), GLC3B (1p36.2-36.1), GLC3C (14q24.3), and GLC3D (14q24.2-24.3), and two causative genes, cytochrome P450 family 1 subfamily B member 1 (*CYP1B1*; OMIM 601771) and latent transforming growth factor-beta binding protein 2 (*LTBP2*; OMIM 602091), have been identified for PCG thus far [19-25]. Pathogenic mutations in *CYP1B1* are the most common cause of PCG and are responsible for 27% of sporadic and 87% of familial PCG cases worldwide [26]. To date, a total of nine mutations, including missense and frameshift, have been identified in *LTBP2* responsible for PCG [20,22,27-29]. Recently, an autosomal dominant model of PCG with variable expression was identified in a fifth locus, GLC3E (9p21.2) harboring mutations in the tunica

Correspondence to: S. Amer Riazuddin, The Wilmer Eye Institute, Johns Hopkins University School of Medicine, 600 N. Wolfe Street; Maumenee 809, Baltimore MD 21287; email: riazuddin@jhmi.edu

TABLE 1. CLINICAL CHARACTERISTICS OF AFFECTED INDIVIDUALS OF PKGL076, PKGL015 AND PKGL042.

Family ID	Individual ID	Age at Enrollment	Max. IOP (OD/OS)	CD Ratio (OD/OS)	VA(OD/OS)	Corneal Diameter (B/L)	Other Clinical findings
PKGL076	7	3 Years	36/26	NV/NV	PL/PL	Increased	B/L Bu, CE, CH
PKGL076	8	6.5 Years	28/24	NV/NV	PL/CF	>13mm	B/L Mc, B/L NY.
PKGL076	9	16 Years	NA	0.6/0.4	NPL/PL	Increased	B/L Bu, B/L MF
PKGL015	12	6 Years	40/21	1.0/NV	CF/NPL	NA	Bu, CE
PKGL015	15	5 Years	NV/36	NV/0.9	CF	NA	Only Left Eye, FT
PKGL015	17	8 Years	NA	1.0/NV	CF	NA	Only Right eye, Ap, PI
PKGL042	9	16 years	36/NV	1.0/NV	HM/HM	Increased	Bu, CO
PKGL042	10	12 years	NA	NV/NV	PL/PL	Increased	B/L Bu, B/L CO
PKGL042	11	14 years	24/22	0.7/0.4	PL/HM	13/14mm	B/L Bu, CO, B/L NY.

IOP: intraocular pressure; OD: oculus dexter; OS: oculus sinister; CD Ratio: cup to disc ratio; VA: visual acuity; NV: no view; PL: light perception; NPL: no light perception; HM: hand movement; CF: counting fingers; B/L: bilateral; Bu: buphthalmos; CH: corneal haze; CE: corneal edema; NY: nystagmus; Mc: megalocornea; MF: myopic fundus; Ap: Aphakia; PI: peripheral Iridectomy; FT: Failed trabeculectomy, CO: corneal opacity.

interna endothelial cell kinase (*TEK*; OMIM 600221) gene [12]. These findings were consistent with previous findings in terms of high penetrance as well as variable expression of the paired-like homeodomain transcription factor 2 (*PITX2*; OMIM 601542), forkhead box C1 (*FOXC1*; OMIM 601090), paired box gene 6 (*PAX6*; OMIM 607108), and optic atrophy 1 (*OPA1*; OMIM 605290) genes responsible for developmental glaucoma in an autosomal dominant inheritance pattern [30-36].

A total of 30 familial cases affected with PCG were identified and recruited from different cities in Pakistan. Of these cases, 23 families were linked to *CYP1B1* with a total of 11 mutations reported previously, and three families showed linkage to *LTBP2* [37]. In the present study, we report three novel mutations, including two missense and a frameshift in the *LTBP2* gene, in three consanguineous families with PCG who were negative for mutations in *CYP1B1*.

METHODS

Subject recruitment and clinical evaluation: Patients affected with PCG were identified and recruited from pediatric departments of Layton Rahmatulla Benevolent Trust (LRBT) and Children's Hospital Lahore. Informed written consent was obtained from all participating family members consistent with the tenets of the Declaration of Helsinki and ARVO (Association for Research in Vision and Ophthalmology) statement on human subjects as well. This study was approved by the Institutional Review Board (IRB) of the National Eye Institute (Bethesda, MD), the Johns Hopkins

University School of Medicine (Baltimore, MD), and the National Centre of Excellence in Molecular Biology (Lahore, Pakistan).

A detailed medical and clinical history was obtained by interviewing all members of the family. Ophthalmic examination including slit-lamp microscopy was performed at the LRBT Hospital (Lahore, Pakistan). Elevated IOP (>16 mmHg for children and >21 mmHg for adults), corneal edema, increased corneal diameter (>12.0 mm), and a large cup to disc ratio (C/D ratio) were inclusion criteria for the patients.

Approximately 10 ml of blood was drawn from all participating family members, and the samples were stored in 50 ml Sterilin Falcon tubes with 20 mM EDTA. Genomic DNA was extracted as previously described [38,39].

Exclusion and linkage analysis: The known or reported loci or genes associated with PCG were screened by genotyping 16 polymorphic short tandem repeat (STR) markers spanning *GLC3A/CYP1B1* (D2S2163, D2S177, D2S1346, D2S2331), *GLC3B* (D1S228, D1S402, D1S507, D1S2672), *GLC3C* (D14S274, D14S63, D14S258), and *GLC3D/LTBP2* (D14S43, D14S1036, D14S61, D14S59, D14S74). Amplification reactions for the exclusion analysis were performed as previously described [38,39]. The amplified products from each DNA sample were mixed with a loading cocktail containing 400 HD size standards (Applied Biosystems, Mountain View, CA) and resolved on an ABI 3100 Genetic Analyzer (Applied Biosystems). Genotypes were assigned with GeneMapper software (Applied Biosystems).

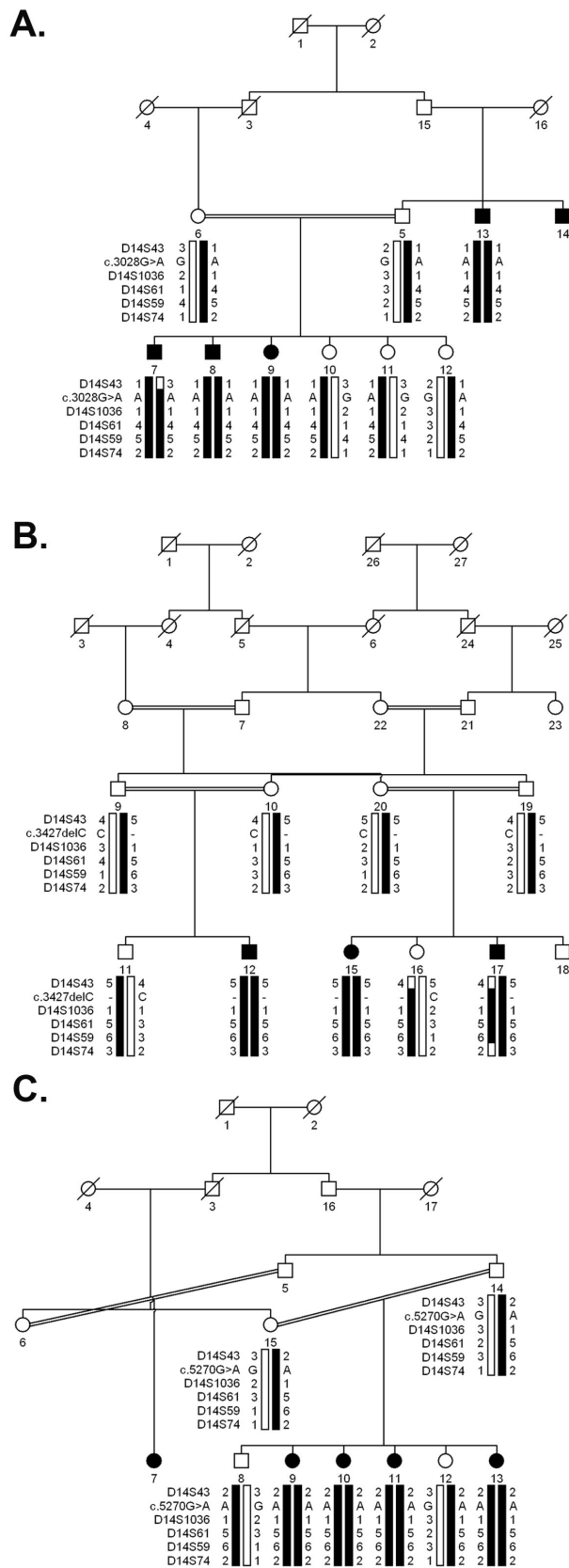


Figure 1. Pedigree drawing of families harboring mutations in *LTBP2* with the haplotypes of alleles for chromosome 14q24.2–24.3 micro-satellite markers. **A:** PKGL076. **B:** PKGL015. **C:** PKGL042. Alleles forming the risk haplotype are shaded black, and alleles not cosegregating with primary congenital glaucoma are shown in white. Square: male; circle: female; filled symbol: affected individual; the double line between individuals: consanguineous marriage; diagonal line through a symbol: deceased family member.

TABLE 2. TWO-POINT LOD SCORES OF PKGL076, PKGL015, AND PKGL042 FOR ALLELES OF CHROMOSOME 14q24.2-24.3 MICROSATELLITE MARKERS.

Markers	cM	Mb	0	0.01	0.03	0.05	0.07	0.09	0.1	0.2	0.3	Z _{max}	θ _{max}
PKGL076													
D14S43	84.16	74.47	-∞	0.79	1.14	1.24	1.26	1.24	1.22	0.89	0.47	1.26	0.07
D14S1036	84.69	75.33	2.86	2.79	2.65	2.52	2.38	2.24	2.17	1.48	0.82	2.86	0
D14S61	86.29	75.86	2.86	2.79	2.65	2.52	2.38	2.24	2.17	1.48	0.82	2.86	0
D14S59	87.36	77.6	2.86	2.79	2.65	2.52	2.38	2.24	2.17	1.48	0.82	2.86	0
D14S74	87.36	78.19	2.73	2.67	2.53	2.39	2.26	2.12	2.05	1.36	0.7	2.73	0
PKGL015													
D14S43	84.16	74.47	-∞	-0.35	0.06	0.22	0.29	0.33	0.34	0.13	0	0.35	0.1
D14S1036	84.69	75.33	2	1.96	1.88	1.8	1.72	1.63	1.59	0.59	0	2	0
D14S61	86.29	75.86	2.73	2.67	2.53	2.39	2.25	2.11	2.05	0.7	0	2.73	0
D14S59	87.36	77.6	2.8	2.73	2.6	2.48	2.34	2.21	2.14	0.83	0	2.8	0
D14S74	87.36	78.19	-∞	0.6	0.96	1.06	1.09	1.08	1.07	0.4	0	1.09	0.07
PKGL042													
D14S43	84.16	74.47	2.75	2.7	2.58	2.46	2.34	2.21	2.15	1.54	0.91	2.75	0
D14S1036	84.69	75.33	2.92	2.86	2.74	2.62	2.5	2.38	2.32	1.7	1.08	2.92	0
D14S61	86.29	75.86	2.92	2.86	2.74	2.62	2.5	2.38	2.32	1.7	1.08	2.92	0
D14S59	87.36	77.6	2.92	2.86	2.74	2.62	2.5	2.38	2.32	1.7	1.08	2.92	0
D14S74	87.36	78.19	2.75	2.7	2.58	2.46	2.34	2.21	2.15	1.54	0.91	2.75	0

LOD: logarithm of odds

Two-point linkage analyses were performed using the FASTLINK version of MLINK from the LINKAGE Program Package (provided in the public domain by the Human Genome Mapping Project Resources Centre, Cambridge, UK) [40,41]. Maximum logarithm of odds (LOD) scores were calculated using PLINK (Shaun Purcell, Boston, MA). PCG was analyzed as a fully penetrant trait with an affected allele frequency of 0.001. The marker order and distances between the markers were obtained from the NCBI (National Center

for Biotechnology Information, Bethesda, MD) chromosome 14 sequence maps.

Sanger sequencing for mutation screening: Thirty-four primer pairs for *LTBP2* were designed by using the Primer3 program. The PCR amplification was performed in 10 µl volume with 20 ng of genomic DNA. The reaction consisted of denaturation step at 95 °C for 5 min followed by a two-step touchdown procedure. The first step of 10 cycles consisted of denaturation at 95 °C for 30 s, followed by a primer set specific annealing for 30 s (annealing temperature decrease

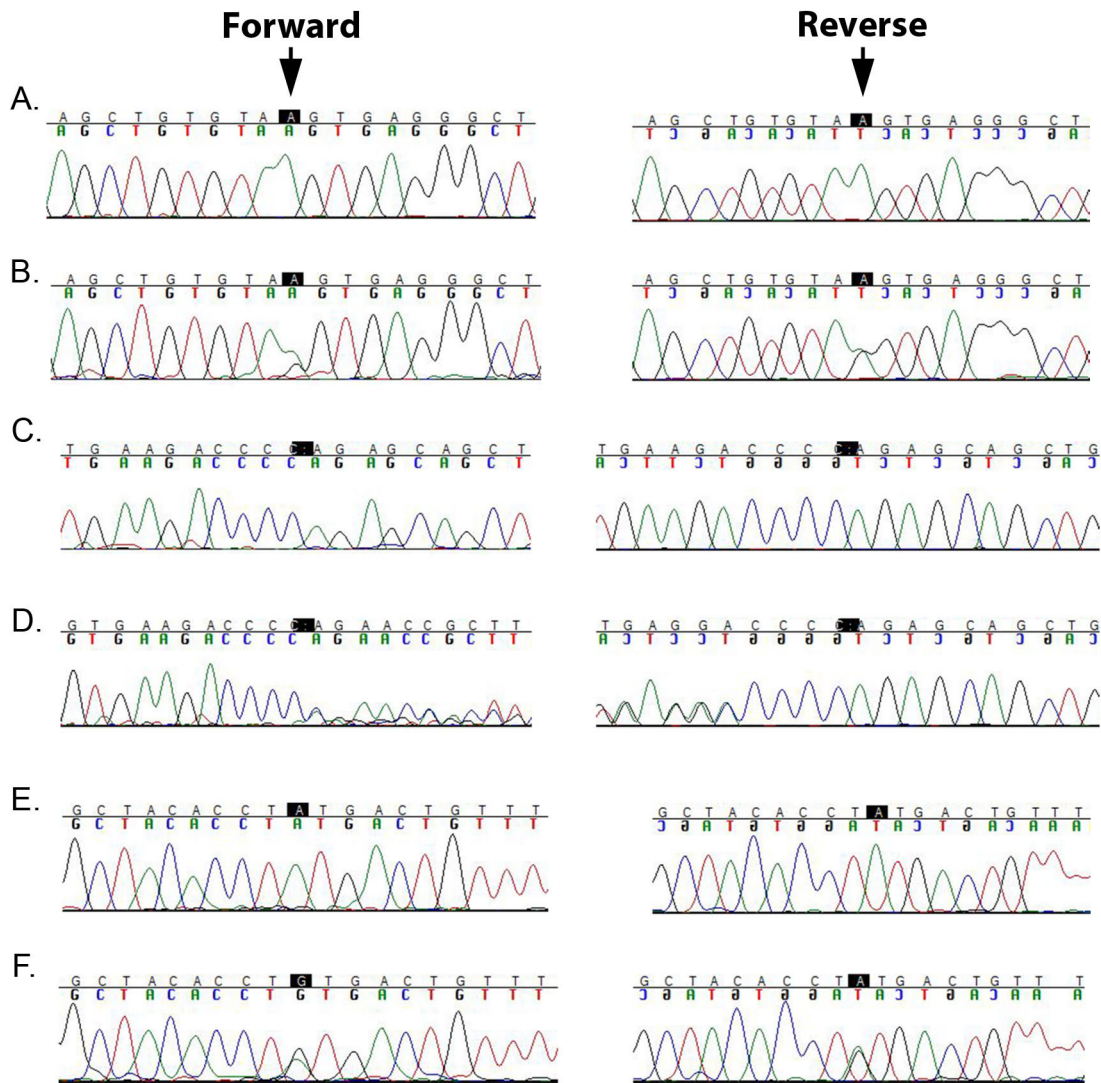


Figure 2. Bidirectional Sanger sequencing identified pathogenic mutations in *LTBP2*. Forward and reverse sequence chromatograms. **A:** Affected individual 7 of PKGL076 homozygous for a novel missense mutation c.3028G>A (p.Asp1010Asn). **B:** Unaffected individual 5 heterozygous carrier of PKGL076 for c.3028G>A (p.Asp1010Asn). **C:** Affected individual 15 of PKGL015 homozygous for a novel frameshift mutation c.3427delC (p.Gln1143Argfs*35). **D:** Unaffected individual 11 heterozygous carrier of PKGL015 for c.3427delC (p.Q1143Rfs*35). **E:** Affected individual 9 of PKGL042 homozygous for a novel missense mutation c.5270G>A (p.Cys1757Tyr). **F:** Unaffected individual 14 heterozygous carrier of PKGL042 for c.5270G>A (p.Cys1757Tyr).

by 1 °C per cycle) and elongation at 72 °C for 45 s. The second step of 30 cycles consisted of denaturation at 95 °C for 30 s followed by annealing (annealing temperature -10 °C) for 30 s and elongation at 72 °C for 45 s, followed by a final elongation at 72 °C for 10 min [42]. The PCR primers for each exon were used for bidirectional sequencing with the BigDye Terminator Ready Reaction mix, according to

the manufacturer’s instructions (Thermo Fisher Scientific, Waltham, MA). Sequencing products were dissolved in 10 µl of formamide (Applied Biosystems) and resolved on an ABI PRISM 3100 Genetic Analyzer (Applied Biosystems). Sequencing results were assembled with ABI PRISM sequencing analysis software, version 3.7, and analyzed with SeqScape software (Applied Biosystems).

Human	S ₁₀₀₇	C ₁₀₀₈	V ₁₀₀₉	D ₁₀₁₀	V ₁₀₁₁	N ₁₀₁₂	E ₁₀₁₃	G ₁₇₅₄	Y ₁₇₅₅	T ₁₇₅₆	C ₁₇₅₇	D ₁₇₅₈	C ₁₇₅₉	F ₁₇₆₀
Chimp	S	C	V	D	V	N	E	G	Y	T	C	D	C	F
Gorilla	S	C	V	D	V	N	E	G	Y	T	C	D	C	F
Orangutan	S	C	V	D	V	N	E	G	Y	T	C	D	C	F
Gibbon	S	C	V	D	V	N	E	G	Y	T	C	D	C	F
Rhesus	S	C	V	D	V	N	E	G	Y	T	C	D	C	F
Crab-eating macaque	S	C	V	D	V	N	E	G	Y	T	C	D	C	F
Baboon	S	C	V	D	V	N	E	G	Y	T	C	D	C	F
Green monkey	S	C	V	D	V	N	E	G	Y	T	C	D	C	F
Marmoset	S	C	V	D	V	N	E	G	Y	T	C	D	C	F
Squirrel monkey	S	C	V	D	V	N	E	G	Y	T	C	D	C	F
Chinese tree shrew	S	C	V	D	V	N	E	G	Y	T	C	D	C	F
Prairie vole	S	C	V	D	V	N	E	G	Y	T	C	D	C	F
Chinese hamster	S	C	V	D	V	N	E	G	Y	T	C	D	C	F
Mouse	S	C	V	D	V	N	E	G	Y	T	C	D	C	F
Naked mole rat	S	C	V	D	V	N	E	G	Y	T	C	D	C	F
Guinea pig	S	C	V	D	V	N	E	G	Y	T	C	D	C	F
Brush tailed rat	S	C	V	D	V	N	E	G	Y	T	C	D	C	F
Rabbit	S	C	V	D	V	N	E	G	Y	T	C	D	C	F
Pika	S	C	V	D	V	N	E	G	Y	T	C	D	C	F
Pig	S	C	V	D	V	N	E	G	Y	T	C	D	C	F
Alpaca	S	C	V	D	V	N	E	G	Y	T	C	D	C	F
Bactrian camel	S	C	V	D	V	N	E	G	Y	T	C	D	C	F
Dolphin	S	C	V	D	V	N	E	G	Y	T	C	D	C	F
Killer whale	S	C	V	D	V	N	E	G	Y	T	C	D	C	F
Tibetan antelope	S	C	V	D	V	N	E	G	Y	T	C	D	C	F
Cow	S	C	V	D	V	N	E	G	Y	T	C	D	C	F
Sheep	S	C	V	D	V	N	E	G	Y	T	C	D	C	F
Domestic goat	S	C	V	D	V	N	E	G	Y	T	C	D	C	F
White rhinoceros	S	C	V	D	V	N	E	G	Y	T	C	D	C	F
Cat	S	C	V	D	V	N	E	G	Y	T	C	D	C	F
Dog	S	C	V	D	V	N	E	G	Y	T	C	D	C	F
Ferret	S	C	V	D	V	N	E	G	Y	T	C	D	C	F
Panda	S	C	V	D	V	N	E	G	Y	T	C	D	C	F
Black flying fox	S	C	V	D	V	N	E	G	Y	T	C	D	C	F
Megabat	S	C	V	D	V	N	E	G	Y	T	C	D	C	F
David's myotis (bat)	S	C	V	D	V	N	E	G	Y	T	C	D	C	F
Big brown bat	S	C	V	D	V	N	E	G	Y	T	C	D	C	F
Shrew	S	C	V	D	V	N	E	G	Y	T	C	D	C	F
Elephant	S	C	V	D	V	N	E	G	Y	T	C	D	C	F
Manatee	S	C	V	D	V	N	E	G	Y	T	C	D	C	F
Cape golden mole	S	C	V	D	V	N	E	G	Y	T	C	D	C	F
Tenrec	S	C	V	D	V	N	E	G	Y	T	C	D	C	F

Figure 3. Sequence alignment of LTBP2 orthologs illustrating the conservation of amino acids aspartic acid at position 1010 and cysteine at position 1757. Red: primates; green: Euarchontoglires; blue: Laurasiatheria; and black: Afrotheria.

Evolutionary conservation and prediction analysis: The evolutionary conservation of mutated amino acids was examined by using the UCSC Genome Browser (<https://genome.ucsc.edu>). The possible effect of substituted amino acid on the structure of the protein was further examined with Sorting Intolerant from Tolerant (SIFT), PolyPhen-2, CONsensus DELETreiousness score of non-synonymous single nucleotide variants (Condel), Mutation Taster, and LoFtool. The Human Splicing Finder (HSF) tool was used to better understand the impact of exonic mutation causing any splicing defects. The novelty of the pathogenic variant was confirmed with the 1000 Genomes, dbSNP, gnomAD, and Exome Variant Server databases and 200 ethnically matched control chromosomes.

RESULTS

In this study, we report three familial cases, PKGL076, PKGL015, and PKGL042, recruited from different cities in Punjab, Pakistan. A detailed history was obtained for affected individuals in each family through family interviews and available medical records. Pedigree and haplotype analysis revealed the disease phenotype segregates with an autosomal recessive pattern. All affected individuals developed the disease symptoms within the first 3 years of life. Affected individuals from these familial cases underwent a detailed ophthalmic examination including slit-lamp biomicroscopy to confirm the diagnosis.

Ophthalmic examination of PKGL076 showed bilateral (B/L) buphthalmos, corneal edema, B/L corneal haze, and an increased corneal diameter (>13 mm) in individual 7. The maximum IOP recorded for this individual was 36/26 mmHg (oculus dexter/oculus sinister [OD/OS]) and visual acuity reduced to the perception of light in both eyes. Individual 8 developed PCG symptoms at 1.5 years of age. Medical records showed B/L buphthalmos, B/L nystagmus, elevated

IOP of 28/24 mmHg (OD/OS), and an increased corneal diameter (>13 mm). Detailed medical examination of individual 9 showed B/L buphthalmos and B/L myopic fundus. Fundoscopy of this affected individual revealed a cup to disc ratio of 0.6/0.4 (OD/OS). Visual acuity was reduced to the perception of light in the left eye whereas the right eye had no perception of light (Table 1).

Detailed medical examination of individual 12 in PKGL015 showed B/L buphthalmos, corneal edema, maximum IOP of 40/21 mmHg (OD/OS), and a C/D ratio of 1.0/ no view (NV; OD/OS). Visual acuity of this affected member was reduced to counting fingers and no perception of light in the right and left eyes, respectively. Medical records of individual 15 showed a maximum IOP of NV/36 mmHg (OD/OS), a C/D ratio of NV/0.9 (OD/OS) and visual acuity reduced to counting fingers. Clinical data of individual 17 showed aphakia, peripheral iridectomy, a C/D ratio of 1.0/NV, and visual acuity reduced to counting fingers only (Table 1).

All affected individuals of PKGL042 exhibited a severe PCG phenotype. Clinical data of affected individual 9 showed B/L buphthalmos and corneal opacity. The maximum IOP recorded was 36/NV mmHg (OD/OS), and the C/D ratio was 1.0/NV (OD/OS). Visual acuity was reduced to hand movement only. Medical records of individual 10 showed B/L buphthalmos, B/L corneal opacity, and an increased corneal diameter (>13 mm). The ophthalmic examination of affected individual 11 revealed a maximum IOP of 24/22 mmHg (OD/OS), a C/D ratio of 0.7/0.4 (OD/OS), and a corneal diameter of 13/14 mm (OD/OS). Additional clinical findings included B/L buphthalmos, corneal opacification, and B/L nystagmus (Table 1).

Initially, linkage analysis was performed on all families for previously reported genes and loci responsible for PCG,

TABLE 3. A LIST OF PREVIOUSLY REPORTED PATHOGENIC MUTATIONS IN LTBP2 RESPONSIBLE FOR PRIMARY CONGENITAL GLAUCOMA.

Nucleotide Change	Protein Change	Exon of LTBP2	Mutation	Ethnicity	Reference
c.331C>T	p.Gln111*	1	Nonsense	Pakistani	[20]
c.412delG	p.Ala138Profs*278	1	Deletion	Pakistani	[20]
c.895C>T	p.Arg299*	4	Nonsense	Gypsy	[20]
c.1243_1256del14	p.Glu415Argfs*596	6	Deletion	Pakistani	[20]
c.1415delC	p.Ser472fs*3	7	Deletion	Iranian	[22]
c.2421G>A	p.Trp807*	14	Nonsense	Indian	[29]
c.4031InsA	p.Asp1345Glyfs*6	27	Insertion	Pakistani	[28]
c.4934G>A	p.Arg1645Glu	34	Missense	Pakistani	[28]
c.5376delC	p.Tyr1793fs*55	36	Deletion	Iranian	[22]

Note: the reference numbers correspond to the bibliography of the manuscript.

including the GLC3D locus on chromosome 14q24.2–24.3. All available members of the families (PKGL076, PKGL015, and PKGL042) were genotyped for microsatellite markers (D14S63, D14S258, D14S43, D14S1036, D14S61, D14S59, and D14S74) flanking the GLC3D locus. The haplotype analysis of chromosome 14 markers in all families revealed the linkage of the PCG phenotype to the GLC3D locus (Figure 1). Maximum two-point LOD scores of 2.86, 2.8 and 2.92, at recombination fraction $\theta=0$, were obtained for the D14S1036, D14S59, and D14S59 markers, for PKGL076, PKGL015, and PKGL042, respectively (Table 2).

Subsequently, all 36 coding exons, exon–intron boundaries along with 5' and 3' untranslated regions (UTRs) of *LTBP2* were sequenced in all available family members of PKGL076, PKGL015, and PKGL042. In PKGL076, a novel homozygous missense mutation (c.3028G>A) was identified in exon 19 of *LTBP2* that results in the substitution of asparagine for aspartic acid at position 1010 (p.Asp1010Asn; Figure 2A,B). In PKGL015, bidirectional sequencing of the *LTBP2* gene identified a novel single-base deletion at the coding nucleotide position: c.3427delC (p.Q1143Rfs*35; Figure 2C,D). In PKGL042, a novel guanine to adenine transition mutation (c.5270G>A) was identified in exon 35 which results in the substitution of tyrosine for cysteine at position 1757 (p.Cys1757Tyr; Figure 2E,F). All three mutations showed complete segregation with the PCG phenotype in the respective families and were absent in 200 ethnically matched control chromosomes. Moreover, both missense mutations (c.3028G>A and c.5270G>A) were absent from the Exome Variant Server (EVS), Genome Aggregation Database (gnomAD), dbSNP database, and 1000 Genomes database whereas c.3427delC has been reported in ExAC and gnomAD with a minor allele frequency (MAF) of 0.000008258 and 0.000003981, respectively.

Evolutionary conservation analysis showed high conservation of both residues (Asp1010 and Cys1757) among primates, placental mammals, and vertebrates (Figure 3). The PolyPhen-2, SIFT, LoFtool, and Condel analyses predicted the p.D1010N mutation to be deleterious to the functional and enzymatic activity of the *LTBP2* protein with scores of 1.0000, 0.0000, 0.0599, and 0.9450, respectively. MutationTaster also predicted this mutation to be disease-causing affecting the protein features. In silico analysis predicted that the p.C1757Y mutation would be damaging to the protein function by providing maximum scores of 0.0000, 1.0000, 0.9450, 0.0599, and 194.00 for SIFT, PolyPhen-2, Condel, LoFtool, and MutationTaster, respectively. MutationTaster also provided the conservation of the wild-type nucleotide (g.111113G) based on multiple alignments of genome

sequences of 46 different species. MutationTaster predicted g.111113G to be highly conserved with maximum PhastCons and phyloP scores of 1.000 and 5.924, respectively.

DISCUSSION

In the present study, we identified three novel pathogenic mutations in the *LTBP2* gene in three consanguineous families with PCG (PKGL076, PKGL015, and PKGL042) from Punjab, Pakistan. The homozygous substitution (c.3028G>A; p. Asp1010Asn) identified in PKGL076 occurs within the splice donor site of intron 19, and most likely will perturb the normal splicing pattern of the *LTBP2* protein. We used HSF, an online bioinformatics tool, to predict the effect of c.3028G>A on *LTBP2* mRNA splicing. The HSF analysis generated consensus values of 74.68 and 45.73 for the wild-type (c.3028G) and mutant (c.3028A) nucleotides, respectively. The predicted consensus deviation value of -38.77% for c.3028G>A suggests the loss of the wild-type donor splice site. In parallel, HSF also detected the activation of an exonic cryptic splice acceptor site using the adenine nucleotide (c.3028G>A) in exon 19. The algorithm predicted consensus values of 37.26 and 66.20 for the wild-type (c.3028G) and the new cryptic splice site (c.3028A), respectively. The predicted consensus value deviation of $+77.67\%$ for the new exonic splice acceptor site suggests the loss of the wild-type splice donor site that would result in a frameshift and eventually, would lead to a premature stop codon in the mutant protein. Sanger sequencing of the *LTBP2* gene identified a novel homozygous single-base deletion at c.3427delC in all affected members of PKGL015. This single nucleotide deletion in exon 23 substitutes the amino acid glutamine with arginine at codon 1143 (p.Gln1143Argfs*35), causing a frameshift mutation. This frameshift resulted in truncating the open reading frame of the *LTBP2* protein by creating a premature stop codon, 35 amino acids downstream after the last original amino acid P1142. As a result of this frameshift mutation, a truncated protein of 1,176 amino acids was produced of which only the first 1,142 amino acids were similar to the wild-type *LTBP2* protein. These frameshift mutations change the amino acid composition of the *LTBP2* enzyme which, as a result, renders the functional inactivity of the protein by changing its primary, secondary, and tertiary structures.

We identified the second novel substitution (c.5270G>A) resulting in the substitution of tyrosine for cysteine at position 1757 (p.Cys1757Tyr) in epidermal growth factor (EGF)-like domain 19 of *LTBP2*. The high conservation of cysteine and the flanking amino acids indicates an important role in the structural and functional stability of the *LTBP2* protein. Cysteine, a nonpolar hydrophobic amino acid, involves the

formation of intrachain disulfide bonds. MutationTaster-based in silico analysis ranked p.Cys1757Tyr as disease-causing and predicted the potential loss of EGF-like domain 19 and EGF-like domain 20 and subsequent downstream disulfide bond formations in the mutant LTBP2 protein. In conclusion, the substitution of cysteine with tyrosine will result in the loss of intrachain disulfide bonds and ultimately, disrupts the proper folding and the normal functioning of the LTBP2 protein.

LTBP2 has 36 exons and encodes for an 1,821 amino acid protein [43,44], that belongs to a superfamily of extracellular matrix LTBP proteins and fibrillins comprised of EGF-like domains, transforming growth factor β (TGF- β) binding protein (TB)-like motifs [22,45-47]. *LTBP2* protein is an extracellular matrix protein and has a presumed role in cell adhesion and elastin microfibril assembly [48-52]. The association of *LTBP2* with microfibrils and its noticeable presence in elastic tissues has been reported [53].

The *LTBP2* protein is expressed in the trabecular meshwork, and is important in the regulation of IOP and for the development of ciliary zonules and the anterior chamber, as well as the production of aqueous humor [54]. Furthermore, *LTBP2* is highly expressed in tissues rich in elastic fibers, i.e., arteries, and lungs [55]. Mutations in *LTBP2* were identified to cause PCG in families and patients from Pakistani, Gypsy, Iranian, and Indian populations [20,22,27-29].

PCG is a genetically heterogeneous disease with variable patterns and expressivity. The most common clinical features persistent with PCG are elevated IOP, buphthalmos, increased corneal diameter, corneal edema or haze, and reduced visual acuity. The clinical presentation of PCG cases harboring mutations in *CYP1B1* or *LTBP2* is similar with the exception of a few subtle phenotypic differences. For instance, in a family reported from Pakistani population, one of the patients had a persistent pupillary membrane and had a bilateral subluxated lens. The other patient in the same family had microspherophakia and iridogoniodysgenesis in addition to the cardinal symptoms of PCG, whereas the second family had typical symptoms [28]. Furthermore, in a recent study of 36 large consanguineous Pakistani families, several patients affected by PCG had classical or typical symptoms (reduced vision and corneal haze) in only one eye which is in direct contrast with the present study in which all the individuals were affected bilaterally in the first 3 years of life. Similarly, one affected member of the family had high IOP but no corneal haze or vision impairment, which is also in slight contrast to the present study in which all affected individuals have much reduced visual acuity along with corneal haze, corneal edema, or megalocornea [56].

In summary, we have identified three novel *LTBP2* mutations, c.3028G>A (p. Asp1010Asn), c.3427delC (p.Gln1143Argfs*35), and c.5270G>A (p.Cys1757Tyr), in three Pakistani familial cases with PCG. Thus far, only nine mutations in *LTBP2* have been reported in patients with PCG of Pakistani, Gypsy, Iranian, and Indian descent which suggests that these mutations are a relatively rare cause of PCG (Table 3). The present study results along with those of previous studies suggest that mutations in *LTBP2* are a plausible cause of ocular anomalies that may lead to elevated IOP and eventually cause PCG.

ACKNOWLEDGMENTS

The authors are thankful to all enrolled members for their participation in this study. This study was funded, in part, by King Khaled Eye Specialist Hospital-Johns Hopkins University collaboration grant and the Higher Education Commission (HEC), Islamabad, Pakistan.

REFERENCES

1. Quigley HA, Broman AT. The number of people with glaucoma worldwide in 2010 and 2020. *Br J Ophthalmol* 2006; 90:262-7. [PMID: 16488940].
2. Vasilioi V, Gonzalez FJ. Role of CYP1B1 in glaucoma. *Annu Rev Pharmacol Toxicol* 2008; 48:333-358-[PMID: 17914928].
3. Sarfarazi M, Stoilov I, Schenkman JB. Genetics and biochemistry of primary congenital glaucoma. *Ophthalmol Clin North Am* 2003; 16:543-54. vi.[PMID: 14740995].
4. Surgucheva I, Surguchov A. Expression of caveolin in trabecular meshwork cells and its possible implication in pathogenesis of primary open angle glaucoma. *Mol Vis* 2011; 17:2878-[PMID: 22128235].
5. Lewis CJ, Hedberg-Buenz A, DeLuca AP, Stone EM, Alward WL, Fingert JH. Primary congenital and developmental glaucomas. *Hum Mol Genet* 2017; 26:R28-36. [PMID: 28549150].
6. Beck AD. Primary congenital glaucoma in the developing world. *Ophthalmology* 2011; 118:229-230-[PMID: 21292107].
7. Ho CL, Walton DS. Primary megalocornea: clinical features for differentiation from infantile glaucoma. *J Pediatr Ophthalmol Strabismus* 2004; 41:11-7-[PMID: 14974829].
8. Moore DB, Tomkins O, Ben-Zion I. A review of primary congenital glaucoma in the developing world. *Surv Ophthalmol* 2013; 58:278-85-[PMID: 23465868].
9. Nagao K, Noel LP, Noel ME, Walton DS. The spontaneous resolution of primary congenital glaucoma. *J Pediatr Ophthalmol Strabismus* 2009; 46:139-43-[PMID: 19496494].

10. Sharafieh H, Child AH, Sarfarazi M, Traboulsi EI. Molecular genetics of primary congenital glaucoma.; in *Genetic Disease of the Eye.*: OUP USA, 2011, pp 295-307.
11. Bejjani BA, Stockton DW, Lewis RA, Tomey KF, Dueker DK, Jabak M, Astle WF, Lupski JR. Multiple CYP1B1 mutations and incomplete penetrance in an inbred population segregating primary congenital glaucoma suggest frequent de novo events and a dominant modifier locus. *Hum Mol Genet* 2000; 9:367-74-[\[PMID: 10655546\]](#).
12. Souma T, Tompson SW, Thomson BR, Siggs OM, Kizhatil K, Yamaguchi S, Feng L, Limviphuvadh V, Whisenhunt KN, Maurer-Stroh S, Yanovitch TL, Kalaydjieva L, Azmanov DN, Finzi S, Mauri L, Javadiyan S, Souzeau E, Zhou T, Hewitt AW, Kloss B, Burdon KP, Mackey DA, Allen KF, Ruddle JB, Lim SH, Rozen S, Tran-Viet KN, Liu X, John S, Wiggs JL, Pasutto F, Craig JE, Jin J, Quaggin SE, Young TL. Angiopoietin receptor TEK mutations underlie primary congenital glaucoma with variable expressivity. *J Clin Invest* 2016; 126:2575-87. [\[PMID: 27270174\]](#).
13. Allen KF, Gaier ED, Wiggs JL. Genetics of primary inherited disorders of the optic nerve: clinical applications. *Cold Spring Harb Perspect Med* 2015; 5:a017277-[\[PMID: 26134840\]](#).
14. Cascella R, Strafella C, Germani C, Novelli G, Ricci F, Zampatti S, Giardina E. The genetics and the genomics of primary congenital glaucoma. *BioMed Res Int* 2015; xxx:321291-[\[PMID: 26451367\]](#).
15. Fan BJ, Wiggs JL. Glaucoma: genes, phenotypes, and new directions for therapy. *J Clin Invest* 2010; 120:3064-72-[\[PMID: 20811162\]](#).
16. Kaur K, Reddy AB, Mukhopadhyay A, Mandal AK, Hasnain SE, Ray K, Thomas R, Balasubramanian D, Chakrabarti S. Myocilin gene implicated in primary congenital glaucoma. *Clin Genet* 2005; 67:335-40. [\[PMID: 15733270\]](#).
17. Khan AO. Genetics of primary glaucoma. *Curr Opin Ophthalmol* 2011; 22:347-55. .
18. Wang R, Wiggs JL. Common and rare genetic risk factors for glaucoma. *Cold Spring Harb Perspect Med* 2014; 4:a017244-.
19. Akarsu AN, Turacli ME, Aktan SG, Barsoum-Homsy M, Chevrette L, Sayli BS, Sarfarazi M. A second locus (GLC3B) for primary congenital glaucoma (Buphthalmos) maps to the 1p36 region. *Hum Mol Genet* 1996; 5:1199-203. [\[PMID: 8842741\]](#).
20. Ali M, McKibbin M, Booth A, Parry DA, Jain P, Riazuddin SA, Hejtmancik JF, Khan SN, Firasat S, Shires M, Gilmour DF, Towns K, Murphy AL, Azmanov D, Tournev I, Cherninkova S, Jafri H, Raashid Y, Toomes C, Craig J, Mackey DA, Kalaydjieva L, Riazuddin S, Inglehearn CF. Null mutations in LTBP2 cause primary congenital glaucoma. *Am J Hum Genet* 2009; 84:664-71. [\[PMID: 19361779\]](#).
21. Firasat S, Riazuddin SA, Hejtmancik JF, Riazuddin S. Primary congenital glaucoma localizes to chromosome 14q24.2-24.3 in two consanguineous Pakistani families. *Mol Vis* 2008; 14:1659-65. .
22. Narooie-Nejad M, Paylakhi SH, Shojae S, Fazlali Z, Rezaei Kanavi M, Nilforushan N, Yazdani S, Babrzadeh F, Suri F, Ronaghi M. Loss of function mutations in the gene encoding latent transforming growth factor beta binding protein 2, LTBP2, cause primary congenital glaucoma. *Hum Mol Genet* 2009; 18:3969-77-[\[PMID: 19656777\]](#).
23. Sarfarazi M, Akarsu AN, Hossain A, Turacli ME, Aktan SG, Barsoum-Homsy M, Chevrette L, Sayli BS. Assignment of a locus (GLC3A) for primary congenital glaucoma (Buphthalmos) to 2p21 and evidence for genetic heterogeneity. *Genomics* 1995; 30:171-7. [\[PMID: 8586416\]](#).
24. Stoilov IR, Sarfarazi M. The third genetic locus (GLC3C) for primary congenital glaucoma (PCG) maps to chromosome 14q24.3. *Invest Ophthalmol Vis Sci* 2002; 43:3015-.
25. Stoilov I, Akarsu AN, Sarfarazi M. Identification of three different truncating mutations in cytochrome P4501B1 (CYP1B1) as the principal cause of primary congenital glaucoma (Buphthalmos) in families linked to the GLC3A locus on chromosome 2p21. *Hum Mol Genet* 1997; 6:641-7. [\[PMID: 9097971\]](#).
26. Sarfarazi M, Stoilov I. Molecular genetics of primary congenital glaucoma. *Eye (Lond)* 2000; 14:Pt 3B422-8. [\[PMID: 11026969\]](#).
27. Azmanov DN, Dimitrova S, Florez L, Cherninkova S, Draganov D, Morar B, Saat R, Juan M, Arostegui JI, Ganguly S, Soodyall H, Chakrabarti S, Padh H, López-Nevot MA, Chernodrinska V, Anguelov B, Majumder P, Angelova L, Kaneva R, Mackey DA, Tournev I, Kalaydjieva L. LTBP2 and CYP1B1 mutations and associated ocular phenotypes in the Roma/Gypsy founder population. *Eur J Hum Genet* 2011; 19:326-33-[\[PMID: 21081970\]](#).
28. Micheal S, Siddiqui SN, Zafar SN, Iqbal A, Khan MI, den Hollander AI. Identification of Novel Variants in LTBP2 and PXDN Using Whole-Exome Sequencing in Developmental and Congenital Glaucoma. *PLoS One* 2016; 11:e0159259-[\[PMID: 27409795\]](#).
29. Yang Y, Zhang L, Li S, Zhu X, Sundaresan P. Candidate Gene Analysis Identifies Mutations in CYP1B1 and LTBP2 in Indian Families with Primary Congenital Glaucoma. *Genet Test Mol Biomarkers* 2017; 21:252-28-[\[PMID: 28384041\]](#).
30. Han J, Thompson-Lowrey AJ, Reiss A, Mayorov V, Jia H, Biousse V, Newman NJ, Brown MD. OPA1 mutations and mitochondrial DNA haplotypes in autosomal dominant optic atrophy. *Genet Med* 2006; 8:217-[\[PMID: 16617242\]](#).
31. Hingorani M, Williamson KA, Moore AT, van Heyningen V. Detailed ophthalmologic evaluation of 43 individuals with PAX6 mutations. *Invest Ophthalmol Vis Sci* 2009; 50:2581-90. [\[PMID: 19218613\]](#).
32. Nishimura DY, Swiderski RE, Alward WL, Searby CC, Patil SR, Bennet SR, Kanis AB, Gastier JM, Stone EM, Sheffield VC. The forkhead transcription factor gene FKHL7 is responsible for glaucoma phenotypes which map to 6p25. *Nat Genet* 1998; 19:140-7. [\[PMID: 9620769\]](#).
33. Nishimura DY, Searby CC, Alward WL, Walton D, Craig JE, Mackey DA, Kawase K, Kanis AB, Patil SR, Stone EM,

- Sheffield VC. A spectrum of FOXC1 mutations suggests gene dosage as a mechanism for developmental defects of the anterior chamber of the eye. *Am J Hum Genet* 2001; 68:364-72. [PMID: 11170889].
34. Semina EV, Reiter R, Leysens NJ, Alward WL, Small KW, Datson NA, Siegel-Bartelt J, Bierke-Nelson D, Bitoun P, Zabel BU, Carey JC, Murray JC. Cloning and characterization of a novel bicoid-related homeobox transcription factor gene, RIEG, involved in Rieger syndrome. *Nat Genet* 1996; 14:392-9. [PMID: 8944018].
 35. Titheradge H, Togneri F, McMullan D, Brueton L, Lim D, Williams D. Axenfeld-Rieger syndrome: further clinical and array delineation of four unrelated patients with a 4q25 microdeletion. *Am J Med Genet A* 2014; 164A:1695-701. [PMID: 24715413].
 36. vis-Silberman N, Kalich T, Oron-Karni V, Marquardt T, Kroeber M, Tamm ER, shery-Padan R. Genetic dissection of Pax6 dosage requirements in the developing mouse eye. *Hum Mol Genet* 2005; 14:2265-76. [PMID: 15987699].
 37. Rauf B, Irum B, Kabir F, Firasat S, Naeem MA, Khan SN, Husnain T, Riazuddin S, Akram J, Riazuddin SA. A spectrum of CYP1B1 mutations associated with primary congenital glaucoma in families of Pakistani descent. *Hum Genome Var* 2016; 3:16021-[PMID: 27508083].
 38. Jiao X, Khan SY, Irum B, Khan AO, Wang Q, Kabir F, Khan AA, Husnain T, Akram J, Riazuddin S, Hejtmancik JF, Riazuddin SA. Missense Mutations in CRYAB Are Liable for Recessive Congenital Cataracts. *PLoS One* 2015; 10:e0137973-[PMID: 26402864].
 39. Jiao X, Kabir F, Irum B, Khan AO, Wang Q, Li D, Khan AA, Husnain T, Akram J, Riazuddin S, Hejtmancik JF, Riazuddin SA. A Common Ancestral Mutation in CRYBB3 Identified in Multiple Consanguineous Families with Congenital Cataracts. *PLoS One* 2016; 11:e0157005-[PMID: 27326458].
 40. Lathrop GM, Lalouel JM. Easy calculations of lod scores and genetic risks on small computers. *Am J Hum Genet* 1984; 36:460-5. [PMID: 6585139].
 41. Schäffer AA, Gupta SK, Shriram K, Cottingham RW. Avoiding recomputation in genetic linkage analysis. *Hum Hered* 1994; 44:225-37. [PMID: 8056435].
 42. Irum B, Khan SY, Ali M, Daud M, Kabir F, Rauf B, Fatima F, Iqbal H, Khan AO, Al OS, Naeem MA, Nasir IA, Khan SN, Husnain T, Riazuddin S, Akram J, Eghrari AO, Riazuddin SA. Deletion at the GCNT2 Locus Causes Autosomal Recessive Congenital Cataracts. *PLoS One* 2016; 11:e0167562-[PMID: 27936067].
 43. Morén A, Olofsson A, Stenman G, Sahlin P, Kanzaki T, Claesson-Welsh L, ten Dijke P, Miyazono K, Heldin C-H. Identification and characterization of LTBP-2, a novel latent transforming growth factor-beta-binding protein. *J Biol Chem* 1994; 269:32469-78-[PMID: 7798248].
 44. ÖKLÜ R, HESKETH R. The latent transforming growth factor β binding protein (LTBP) family. *Biochem J* 2000; •••:352-.
 45. Hyytiäinen M, Penttinen C, Keski-Oja J. Latent TGF- β binding proteins: extracellular matrix association and roles in TGF- β activation. *Crit Rev Clin Lab Sci* 2004; 41:233-64-[PMID: 15307633].
 46. Rifkin DB. Latent transforming growth factor- β (TGF- β) binding proteins: orchestrators of TGF- β availability. *J Biol Chem* 2005; 280:7409-12-[PMID: 15611103].
 47. Sinha S, Heagerty AM, Shuttleworth CA, Kielty CM. Expression of latent TGF-beta binding proteins and association with TGF-beta1 and fibrillin-1 following arterial injury. *Cardiovasc Res* 2002; 53:971-83-[PMID: 11922907].
 48. Fujikawa Y, Yoshida H, Inoue T, Ohbayashi T, Noda K, Von Melchner H, Iwasaka T, Shiojima I, Akama TO, Nakamura T. Latent TGF- β binding protein 2 and 4 have essential overlapping functions in microfibril development. *Sci Rep* 2017; 7:43714-[PMID: 28252045].
 49. Hirai M, Ohbayashi T, Horiguchi M, Okawa K, Hagiwara A, Chien KR, Kita T, Nakamura T. Fibulin-5/DANCE has an elastogenic organizer activity that is abrogated by proteolytic cleavage in vivo. *J Cell Biol* 2007; 176:1061-71-[PMID: 17371835].
 50. Hirani R, Hanssen E, Gibson MA. LTBP-2 specifically interacts with the N-terminal region of fibrillin-1 and competes with LTBP-1 for binding to this microfibrillar protein. *Matrix Biol* 2007; 26:213-23-[PMID: 17293099].
 51. Hyytiäinen M, Keski-Oja J. Latent TGF- β binding protein LTBP-2 decreases fibroblast adhesion to fibronectin. *J Cell Biol* 2003; 163:1363-74-[PMID: 14691143].
 52. Vehviläinen P, Hyytiäinen M, Keski-Oja J. Latent transforming growth factor- β -binding protein 2 is an adhesion protein for melanoma cells. *J Biol Chem* 2003; 278:24705-13-[PMID: 12716902].
 53. Gibson MA, Hatzinikolas G, Davis EC, Baker E, Sutherland GR, Mecham RP. Bovine latent transforming growth factor beta 1-binding protein 2: molecular cloning, identification of tissue isoforms, and immunolocalization to elastin-associated microfibrils. *Mol Cell Biol* 1995; 15:6932-42-[PMID: 8524260].
 54. Shipley JM, Mecham RP, Maus E, Bonadio J, Rosenbloom J, McCarthy RT, Baumann ML, Frankfater C, Segade F, Shapiro SD. Developmental expression of latent transforming growth factor β binding protein 2 and its requirement early in mouse development. *Mol Cell Biol* 2000; 20:4879-87-[PMID: 10848613].
 55. Inoue T, Ohbayashi T, Fujikawa Y, Yoshida H, Akama TO, Noda K, Horiguchi M, Kameyama K, Hata Y, Takahashi K. Latent TGF- β binding protein-2 is essential for the development of ciliary zonule microfibrils. *Hum Mol Genet* 2014; 23:5672-82-[PMID: 24908666].
 56. Rashid M, Yousaf S, Sheikh SA, Sajid Z, Shabbir AS, Kausar T, Tariq N, Usman M, Shaikh RS, Ali M, Bukhari SA, Waryah AM, Qasim M, Riazuddin S, Ahmed ZM. Identities and frequencies of variants in CYP1B1 causing primary congenital glaucoma in Pakistan. *Mol Vis* 2019; 25:144-54. [PMID: 30820150].

Articles are provided courtesy of Emory University and the Zhongshan Ophthalmic Center, Sun Yat-sen University, P.R. China. The print version of this article was created on 24 February 2020. This reflects all typographical corrections and errata to the article through that date. Details of any changes may be found in the online version of the article.